

Nanotube Molecular Transporters: Internalization of Carbon Nanotube–Protein Conjugates into Mammalian Cells

Nadine Wong Shi Kam, Theodore C. Jessop, Paul A. Wender,* and Hongjie Dai*

Department of Chemistry Stanford University, Stanford, California 94305

Received March 10, 2004; E-mail: hdai@stanford.edu; wenderp@stanford.edu

The design of new strategies for the delivery of drugs and molecular probes into cells is necessitated by the poor cellular penetration of many small molecules and an increasing number of macromolecules including proteins and nucleic acids.¹ Strategies in which a poorly permeating drug or probe molecule is covalently attached to a transporter to produce a cell-penetrating conjugate offer a solution to this problem. Several classes of transporters have been investigated including lipids, PEGs, and more recently peptides.^{2–5} The ability of new materials such as nanotubes^{6,7} to serve as biocompatible transporters has received relatively little attention. Thus far, the main activities at this interface of materials and life sciences include functionalization and immobilization of biomolecules on nanotubes for characterization, manipulation, separation, and for device applications such as biosensors.^{8–14} Few reports exist thus far on how carbon nanotubes interact with and affect living systems. Mattson et al. have investigated the growth pattern of neurons on as-grown and functionalized multiwalled nanotubes.¹⁵ Recently, Pantarotto et al. reported the internalization of fluorescently labeled nanotubes into cells with no apparent toxicity effects observed, although without identifying the uptake mechanism.¹⁶ Here, we present our findings on the uptake of single-walled nanotubes (SWNT) and SWNT–streptavidin (a protein with clinical applications in anticancer therapies¹⁷) conjugates into human promyelocytic leukemia (HL60) cells and human T cells (Jurkat) via the endocytosis pathway.

Stable aqueous suspensions of purified, shortened, and functionalized nanotubes were obtained by oxidation and sonication^{9,10} of laser-ablated SWNT. Specifically, SWNTs were refluxed in 2.5 M HNO₃ for two 36-h periods separated by cup-horn sonication for 30 min [see Supporting Information (SI)]. The resulting mixture was then filtered through a 100-nm pore size polycarbonate filter, rinsed, and resuspended in pure water with sonication. Centrifugation (7000 rpm, 5 min) removed larger unreacted impurities from the solution to afford a stable suspension of **1**.

Analysis of **1** by atomic force microscopy revealed mostly short (~100 nm to 1 μm) SWNTs with diameters in the range of 1–5 nm corresponding to mostly isolated individual SWNTs and small bundles (see SI). No significant amounts of particles were observed on the substrate, suggesting good purity of the SWNTs in solution. Zeta potential measurement revealed a surface potential of ~ -75 mV at pH 7 on **1** (see SI), confirming the existence of numerous negatively charged acidic groups at the sidewalls of the nanotubes. In pure water, **1** was stable for extended periods of time and did not agglomerate. In physiological buffer solutions containing ~0.2 M salt, the suspension was less stable and started to aggregate after 2–3 h.

Besides providing a highly stable aqueous suspension of purified, shortened nanotubes, the oxidation/sonication procedure introduced surface carboxylates on the nanotubes for chemical derivatization. Reaction of **1** with EDC and 5-(5-aminopentyl)thioureidyl fluorescein afforded fluorescein-functionalized SWNTs, **2** (Figure 1).

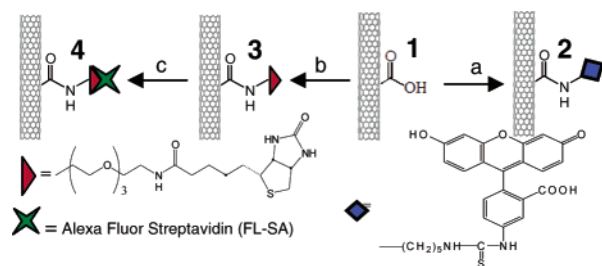


Figure 1. Synthesis and schematic of various SWNT conjugates. (a) EDC, 5-(5-aminopentyl)thioureidyl fluorescein, phosphate buffer; (b) EDC, biotin-LC-PEO-amine, phosphate buffer; (c) fluoresceinated streptavidin.

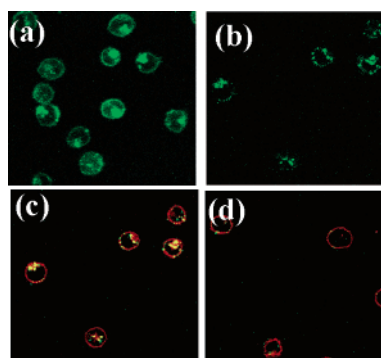


Figure 2. Confocal images of cells after incubation in solutions of SWNT conjugates: (a) after incubation in **2**, (b) after incubation in a mixture of **4** (green due to SA) and the red endocytosis marker FM 4-64 at 37 °C (image shows fluorescence in the green region only), (c) same as b with additional red fluorescence shown due to FM 4-64 stained endosomes, (d) same as b after incubation at 4 °C.

To visualize the interaction of nanotubes with cells, fluorescently labeled nanotubes **2** (0.05 mg/mL SWNT) were incubated with HL60 cells for 1 h at 37 °C. The cells were washed twice, collected by centrifugation, and resuspended in growth medium. Confocal microscopy revealed appreciable fluorescence on the surface and, more importantly, in the cell interior (Figure 2a).

Having discovered the ability of **2** to enter cells, we sought to utilize the nanotubes to carry proteins into cells. Toward this end, **1** was treated with EDC and biotin-LC-PEO-amine followed by dialysis to afford biotin-functionalized SWNTs **3**, which was then incubated with fluoresceinated streptavidin (SA) to afford SWNT–biotin–SA conjugate **4** (Figure 1). To evaluate the ability of nanotubes to enable the cellular uptake of the attached protein, HL60 cells were incubated with **4** as described above. Visualization of the SA revealed intense fluorescence inside the cells (Figure 2b). Importantly, the internalization of SWNT–biotin–SA conjugate **4** illustrates that nanotubes can carry large cargos, in this case SA (MW ≈ 60 kD), and transport them into cells. The uptake of SA was further confirmed by flow cytometry (Figure 3). The fluorescence of cells incubated with SA alone was only slightly

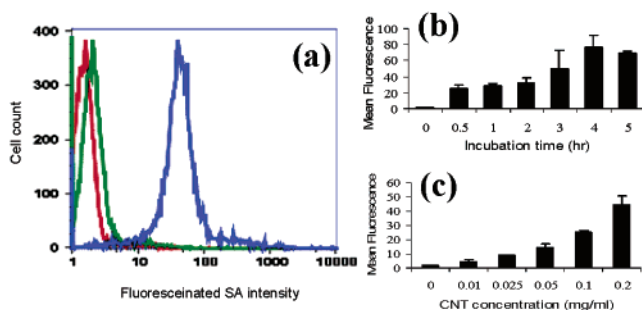


Figure 3. Flow cytometry data. (a) Fluorescence histogram for untreated cells (red curve), cells after 1 h incubation in a solution containing Alexa Fluor-labeled SA only (green curve) and after 1 h incubation in a solution of **4** (blue curve). (b) Mean green fluorescence of cells vs time of incubation in **4** ([SWNT] = 0.05 mg/mL). (c) Mean green fluorescence of cells vs concentration of **4** for 1 h incubation.

greater than the background fluorescence of untreated cells (Figure 3a, green and red curves respectively). We systematically varied the time of cell incubation of **4** ([SWNT] \approx 0.05 mg/mL in the solution) and found uptake increased with longer incubations, up to \sim 4 h (Figure 3b). Upon increasing the concentration of **4** in the incubation solution, we observed a monotonic increase in the cellular fluorescence (Figure 3c).

To examine the potential toxicity of SWNT, HL60 cells were incubated with **1**, **2**, **3**, and **4** (1 h, 0.05 mg/mL tubes), isolated by centrifugation and observed after 24 and 48 h. In the case of **1**, **2**, and **3**, no appreciable cell death was observed (see SI). These results indicate that the functionalized SWNT themselves exhibit little toxicity to HL60 cells.

The SWNT–biotin–SA conjugate **4**, however, was found to cause extensive cell death when examined 48 h after the 1-h incubation with HL60. The degree of cell death was substantial as evidenced by the large amounts of cell debris observed (see SI). We found that the onset of appreciable cell death occurred typically \sim 12 h after the incubation with **4**. To further confirm that the toxicity was due to the delivery of SA into cells, the amount of SA on the SWNT was reduced by decreasing the [SA] used to load the SWNT from 2.5 to 0.0625 μ M (Figure 1c). The observed toxicity was nearly nonexistent at [SA] < 1.25 μ M. The dependence of cell viability on the amount of SA uptake was similar to a previous observation.¹⁷ Consistent with the inability of SA to transverse the cell membrane alone, no toxicity was observed after cells were incubated even in highly concentrated solutions of SA. Significantly, these studies show that the SWNTs not only internalize the protein but the internalized conjugate also elicits a functional dose-dependent response.

The results described above with HL60 cells appear to be general with other cells as well, including Jurkat, Chinese hamster ovary (CHO), and 3T3 fibroblast cell lines. It has been shown that hydrophobic forces are responsible for nonspecific binding between nanotubes and proteins.¹⁴ Although the nanotubes used in the current work contain negatively charged carboxylates along the sidewalls, such groups are likely only present on defect sites along the tubes. The unoxidized areas of the nanotubes may still afford regions of appreciable hydrophobicity. We propose that the nanotubes non-specifically associate with hydrophobic regions of the cell surface and internalize by endocytosis.^{18,19} We detected no green fluorescence from the interior of cells after incubation in **4** at 4 $^{\circ}$ C (Figure

2d), consistent with the blockage of endocytosis at 4 $^{\circ}$ C.^{18,19} Further, we used a red FM 4-64 marker to stain^{19,20} endosomes formed around nanotubes during endocytosis and observed yellow color (Figure 2c) inside cells due to overlapping of green fluorescence (SWNT conjugates) (Figure 2b) and red-stained endosomes (also see SI). This provides a direct evidence for endocytosis of nanotubes conjugates. The nanotubes appear to accumulate in the cytoplasm in the cells after internalization.

In conclusion, we have prepared modified nanotubes and have shown that these can be derivatized to enable attachment of small molecules and proteins. The functionalized SWNT enter nonadherent as well as adherent cell lines (CHO and 3T3) and by themselves are not toxic. While the fluoresceinated protein SA by itself cannot enter cells, it readily enters cells when complexed to a SWNT–biotin transporter, exhibiting dose-dependent cytotoxicity. The uptake pathway is consistent with endocytosis. SWNT could be exploited as molecular transporters for various cargos. The biocompatibility, unique physical, electrical, optical, and mechanical properties of SWNT provide the basis for new classes of materials for drug, protein, and gene delivery applications.

Acknowledgment. Support of this work by grants from CPIMA at Stanford University (H.D.), the National Institutes of Health (P.A.W.: CA NIH CA31841, CA31845), and a Packard Fellowship is acknowledged.

Supporting Information Available: Experimental procedures and additional results and discussions. This material is available free of charge via the Internet at <http://pubs.acs.org>.

References

- (1) Smith, D. A.; van de Waterbeemd, H. *Curr. Opin. Chem. Biol.* **1999**, *3*, 373–378.
- (2) Bendas, G. *Biodrugs* **2001**, *15*, 215–224.
- (3) *Adv. Drug Delivery Rev.* **2002**, *54*.
- (4) Wright, L. R.; J. B. R.; Wender, P. A. *Curr. Protein Peptide Sci.* **2003**, *4*, 105–124.
- (5) Langel, U., Ed.; *Cell-Penetrating Peptides: Processes and Applications*; CRC Press: Boca Raton, Fla, 2002.
- (6) Dresselhaus, M. S.; Dresselhaus, G.; Avouris, P., Eds. *Carbon Nanotubes*; Springer: Berlin, 2001; Vol. 80.
- (7) Dai, H. *Surf. Sci.* **2002**, *500*, 218–241.
- (8) *Acc. Chem. Res.* **2002**, *35*. Special issue on carbon nanotubes.
- (9) Chen, J.; Hammon, M. A.; Hu, H.; Chen, Y. S.; Rao, A. M.; Eklund, P. C.; Haddon, R. C. *Science* **1998**, *282*, 95–98.
- (10) Liu, J.; Rinzler, A. G.; Dai, H.; Hafner, J. H.; Bradley, R. K.; Boul, P. J.; Lu, A.; Iverson, T.; Shelimov, K.; Huffman, C. B.; Rodriguez-Macias, F.; Shon, Y.-S.; Lee, T. R.; Colbert, D. T.; Smalley, R. E. *Science* **1998**, *280*, 1253–1256.
- (11) O'Connell, M. J.; Boul, P.; Ericson, L. M.; Huffman, C.; Wang, Y.; Haroz, E.; Kuper, C.; Tour, J.; Ausman, K.; Smalley, R. E. *Chem. Phys. Lett.* **2001**, *342*, 265–271.
- (12) Chen, R.; Zhang, Y.; Wang, D.; Dai, H. *J. Am. Chem. Soc.* **2001**, *123*, 3838–3839.
- (13) Erlanger, B. F.; Chen, B.; Zhu, M.; Brus, L. E. *Nano Lett.* **2001**, *1*, 465–467.
- (14) Chen, R. J.; Bangsaruntip, S.; Drouvalakis, K. A.; Kam, N. W. S.; Shim, M.; Li, Y. M.; Kim, W.; Utz, P. J.; Dai, H. *J. Proc. Natl. Acad. Sci. U.S.A.* **2003**, *100*, 4984–4989.
- (15) Mattson, M. P.; Haddon, R. C.; Rao, A. M. *J. Mol. Neurosci.* **2000**, *14*, 175–182.
- (16) Pantarotto, D.; Briand, J.; Prato, M.; Bianco, A. *Chem. Commun.* **2004**, *1*, 16–17.
- (17) Hussey, S. L.; Peterson, B. R. *J. Am. Chem. Soc.* **2002**, *124*, 6265–6273.
- (18) Silverstein, S. C.; Steinman, R. M.; Cohn, Z. A. *Annu. Rev. Biochem.* **1977**, *46*, 669–722.
- (19) Vida, T. A.; Emr, S. D. *J. Cell Biol.* **1995**, *128*, 779–792.
- (20) Richard, J. P.; Melikov, K.; Vives, E.; Ramos, C.; Verbeure, B.; Gait, M. J.; Chenomordik, L. V.; Lebleu, B. *J. Biol. Chem.* **2003**, *278*, 585–590.

JA0486059

Nanotube Molecular Transporters: Internalization of Carbon Nanotube-Protein Conjugates into Mammalian Cells

Nadine Wong Shi Kam, Theodore C. Jessop, Paul A. Wender,*
Hongjie Dai*

Experimental

Oxidation and cutting of SWNT. We used a modified oxidation and cutting procedure based on ref. 9 and 10 to treat nanotubes. SWNT (20 mg) grown by laser ablation were mixed with 100 mL of 2.5 M HNO₃. The mixture was refluxed for about 36 h, sonicated with a cup-horn sonicator (Branson Sonifer 450) for 30 min, and then refluxed again for another 36 h. After this treatment, the mixture was filtered through a polycarbonate filter (Whatman, pore size 100 nm), rinsed thoroughly and then re-suspended in pure water by sonication. The aqueous suspension was then centrifuged at 7000 rpm for about 5 min to remove any large un-reacted impurities from the solution.

Nanotube Characterization. Nanotubes undergone the acid treatment above (1) were characterized by atomic force microscopy (AFM) and zeta potential measurements. For AFM, a silica substrate was first treated with (3-aminopropyl)-triethoxysilane (APTES, Aldrich) to render the surface positively charged. A drop of the nanotube suspension was placed on the substrate and kept for 15 min before blow-dry. The substrate was then imaged by an AFM operated in the tapping mode (Digital Instruments). Zeta potential was measured with a ZetaPALS instrument (Brookhaven Instruments Corporation).

Conjugation of Molecules and Proteins to SWNT. Fluorescently labeled SWNT were obtained by reacting the oxidized and cut SWNT with EDC and 5-(5-aminopentyl)thioureidyl fluorescein, dihydrobromide salt (Molecular Probes) to afford SWNT-fluorescein (**2**, Fig. 1a). A suspension of the oxidized and cut SWNT in 0.1M phosphate buffer (pH= 7.4) at a concentration of 0.2 mg/mL were also mixed and reacted overnight with 1-ethyl-3-(3-dimethylamino-propyl) carbodiimide, EDC (10-20 mM) (Fluka chemicals) and biotin-LC-PEO amine (1 mM) (Pierce chemicals) to afford biotinylated SWNT (**3**, Fig. 1b). The resulting solution was then dialyzed against H₂O in a 14-16K MWCO membrane (Spectrapor) for 3 days to remove excess EDC and biotin-LC-PEO amine reagents. The solution was then reacted with 2.5 μ M of Alexa Fluor 488 labeled streptavidin (Molecular Probes) for 1 h to afford SWNT-biotin-SA conjugates (**4**, Fig. 1c, fluorescence due to the Alexa Fluor labeled SA). All of our functionalized SWNT (**2** to **4**) were kept in stock solutions in pure water at a concentration of 0.1 mg/ml

Note that the conjugation of SA to SWNTs in the current work is through biotin. The protein attachment is therefore non-covalent although the SA-biotin binding is quite strong. We are currently devising general methods for attaching proteins on SWNTs in such a way that the proteins can be released from the nanotubes after internalization into cells. A specific approach we are developing is to link proteins to SWNTs via cleavable disulfide bonds.

Incubation of Living Cells in Nanotube Solutions. HL60 and Jurkat cells were both grown in RPMI-1640 cell culture medium (Invitrogen) supplemented with 10% fetal

bovine serum (FBS). Prior to incubation, the cells were collected by centrifugation and resuspended in RPMI medium at a cell density of 3×10^6 cells/mL. Incubation of cells in a nanotube solution was done by mixing 100 μ L of the cell suspension with 100 μ L of a SWNT solution (**2, 3 or 4**) at 37 °C unless otherwise stated. The concentration of SWNT in the incubation solution was ~ 0.05 mg/mL unless otherwise stated, and the incubation duration was always 1 h in 5% CO₂ atmosphere except for time dependent incubation experiments. After incubation, the cells were washed and collected by centrifugation twice, and resuspended in RPMI medium.

Membrane and Endosome Staining of Cells Incubated in Nanotube Solutions. FM 4-64 (Molecular Probes Inc.) is a classical marker used for staining membrane and endosomes.^{19,20} The cell incubations were carried out under similar conditions as discussed in the previous section, except that FM 4-64 (2% v/v) was added to the incubation mixture.

Low Temperature Incubation of Cells with Nanotube Solution. The hour-long incubation of HL-60 cells with carbon nanotubes conjugate was carried out on ice (approximate temperature 4°C). The isolation and rinsing of the cells were achieved as described above.

Confocal Microscopy Imaging of Cells Incubated in Nanotube Solutions. All confocal images were taken immediately after the incubation and washing steps, except

for the cell viability assay described below. 20 μ l of the cell suspension was dropped onto a glass cover slide and imaged by a Zeiss LSM 510 confocal microscope.

Flow Cytometry. Cells were analyzed by a Becton-Dickinson FACScan instrument after incubation in various nanotube solutions. The cell suspension was supplemented with 2% propidium iodide (PI, Fluka chemicals) prior to the measurement. PI is a membrane-impermeable dye and does not stain live cells. It can enter dead cells and intercalate into DNA, thereby selectively staining the dead cells red. We carried out dual detection of red and green fluorescence with the cells. The data presented here represent the mean green fluorescence obtained with a population of 10,000 live cells.

Toxicity and Cell Viability Assay. By cell cytometry: We used the PI staining method to identify dead cells, if any, caused by exposure of the cells to various nanotube solutions. After incubation of cells in a nanotube solution for 1 h, the cells were washed and re-suspended in RPMI medium. The cells were returned to the 37 °C incubator and observed at different time intervals by confocal microscopy method,. For confocal microscopy, the cells were observed at 24 h interval for a period of 48 h. The cells were stained by PI immediately prior to analysis. . For the cell cytometry, the cells were observed immediately after the initial incubation with either conjugate **3** or **4** and the level of cell death was compared with control cells by PI staining

Result and Data

Characterization of Oxidized and Cut SWNT. The acid treatment process used here was modified from previous methods^{9,10} and had three main effects to the starting raw SWNT material, namely, purification, cutting of nanotubes and functionalization of nanotube sidewalls with oxygen groups. The latter affords water solubility and reactivity towards further conjugation of other molecules to the nanotubes. Reflux in nitric acid breaks down amorphous carbon, dissolves some of the metal species in the material and introduces acidic groups at defect sites along the sidewalls of the nanotubes.⁹ The sonication step is known to cut nanotubes into short lengths.¹⁰ The filtration step after the acid treatments removes the acid from the solution and filter out some of the un-reacted graphitic particles existed in the raw laser-oven nanotube material. We characterized the nanotubes that had undergone this treatment by atomic force microscopy (AFM) and zeta-potential measurements. AFM imaging of the materials deposited on a silicon-oxide substrate from a nanotube solution revealed mostly short (~ 100 nm – 1 μ m) SWNT with diameters in the range of $1 - 5$ nm corresponding to mostly isolated individual SWNT and small bundles (S_Fig. 1a). No significant amount of particles was observed on the substrate, suggesting good purity of short SWNT in the nanotube solution. Zeta potential measurement revealed that the cut SWNT exhibited a surface potential of ~ -75 mV at pH 7 (S_Fig. 1b), confirming the existence of highly negatively charged acidic groups at the sidewalls of the nanotubes. In pure water, the oxidized cut SWNT were stable for extended periods of time without agglomeration. The nanotubes were less stable in buffer solutions, and typically aggregated within 2-3 h when exposed to physiological buffer solutions containing ~ 0.2 M salt.

Internalization Mechanism. In order to elucidate the mechanism of entry of the CNT conjugate into the cells, the incubations were carried out in the presence of the membrane and endosome marker FM 4-64 and at low temperatures. FM 4-64 has been previously shown to be an effective marker for endocytosis^{19,20} by specifically staining (red) the endosomes involved in the endocytosis uptake. After the incubation of the cells with both conjugate **4** and FM 4-64, we observed red fluorescence (due to FM 4-64 stained endosomes) around green fluorescence (due to nanotube conjugates) in the cell interior (Fig. 2 in main text, and S_Fig 2 a, c.). The regions stained red and green overlap each other well (yellow regions, S_Fig 2d), thereby indicating that the fluorescence observed from the green CNT-conjugate is located inside the endosomes (red). These results provide direct evidence for the endocytosis uptake pathway.

In order to further confirm endocytosis as the internalization mechanism, we carried out two different incubations of the cells with CNT-conjugate **4** concurrently at 37 °C and 4 °C, both in the presence of the FM 4-64. As shown in Fig. 2d of the main text, the level of fluorescence observed in the low temperature incubation is drastically lower than the 37 °C incubation. Furthermore, the absence of both the red FM 4-64 dye and the green CNT-conjugate from the cell interior indicate that the uptake of both the dye (well established to undergo endocytosis at 37 °C but blocked at 4 °C^{19,20}) and the nanotube conjugate are blocked at 4 °C, thereby confirming that the nanotubes conjugate do get internalized via endocytosis when at 37 °C.

Cell Viability Probed by Microscopy. 48 h after the 1 h incubations of HL60 cells in **3** (SWNT-biotin) and **2** (SWNT-fluorescein) respectively, we did not observe any

appreciable cell death (S_Fig. 3a). Cells were also observed to survive after incubation in solutions of the as-oxidized and cut tubes (without further conjugation to other molecules). These results suggested that the nanotubes themselves (and the ones conjugated with biotin or fluorescein ligands) exhibited little toxicity effects to the HL60 cells.

The SWNT-biotin-SA conjugate (**4**) however, was found to cause extensive cell death when examined 48 h after the hour-long incubation of HL60 in **4**. The degree of cell death was drastic as evidenced by the observation of large amount of disintegrated cell debris (S_Fig. 3b). Since the nanotubes themselves were not toxic as discussed above, and incubation of cells in a solution of SA molecule alone did not lead to any cell death, the observed toxicity after incubation in **4** should be due to the streptavidin cargos transported inside cells via the nanotube carriers. We found that the onset of appreciable cell death occurred typically ~12 h after the incubation in **4** for 1 h and then washing step. We also varied the SA concentration from 2.5 to 0.0625 μM during the SA conjugation step to reduce the amount of proteins attached to the nanotubes, and found that the toxicity effect and cell death were nearly non-existent for $[\text{SA}] < 1.25 \mu\text{M}$. Such cell viability dependence on the amount of SA uptake was similar to a previous observation.¹⁷ Nevertheless the precise cause of cell death due to excess amount of SA internalization remained to be fully understood and could be an interesting subject by itself for further investigations. The drastically reduced cell viability after incubation in **4** did further signal the internalization of the nanotubes-biotin-streptavidin conjugates with the nanotubes acting as efficient transporters. Streptavidin alone was unable to traverse the

cell membrane and therefore no toxicity effects were observed after cells were incubated even in highly concentrated pure SA solutions.

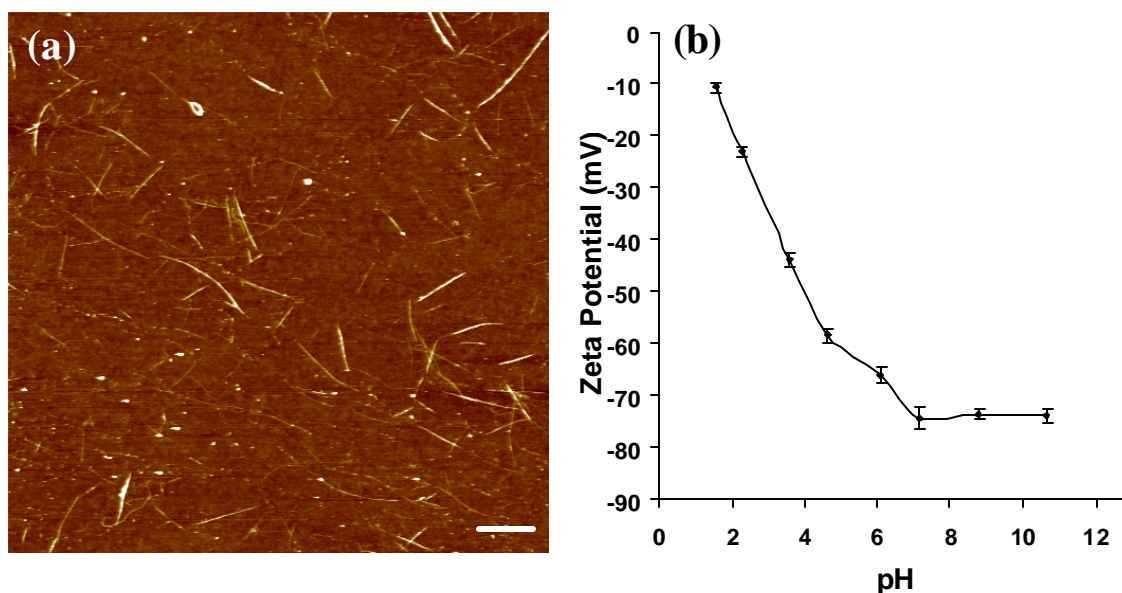
On the Loading of Proteins on SWNTs. The number of proteins attached to nanotubes can be estimated as follows. The defect density on an as-grown SWNT is about 1 per 500 nm in length. However, it has been shown that sonication in acids creates significant amount of defects, and a defect density or carboxylic acid group density of 1 per 10 nm is reasonable (mean distance between defects $l \sim 10$ nm). The specific surface area of a SWNT is $A \sim 1600 \text{ m}^2/\text{g}$. These suggest that the maximum loading of protein on the oxidized tubes is $\sim 2.5 \times 10^{19}$ proteins per gram of SWNTs, or $N = A / (\pi d \times l_d)$, where $d = 2$ nm is the tube diameter. The maximum number of proteins loaded onto 1g of SWNT can therefore be $\sim 40 \text{ } \mu\text{mole/g}$. Our typical protein conjugation experiment involves proteins at concentrations $[\text{SA}] < 2.5 \text{ } \mu\text{M}$ and nanotube concentration of $[\text{SWNT}] = 0.1 \text{ mg/mL}$, which corresponds to $25 \text{ } \mu\text{mole/g}$ (protein/SWNT) and is below the maximum loading capacity of $40 \text{ } \mu\text{mole/g}$. Therefore, varying the concentration of protein in the experimental range ($0.0625 \text{ } \mu\text{M}$ to $2.5 \text{ } \mu\text{M}$) will be effective in changing the loading of proteins on SWNTs, since the nanotubes are in excess relative to the proteins.

Cell Viability Probed by Flow Cytometry. We also monitored cell viability by flow-cytometry. The HL60 cells were monitored by flow cytometry after incubation in conjugate **4** (SWNT-biotin-SA). As shown in S_Figure 4, higher level of PI staining can already be observed in cells immediately after the hour-long incubation with conjugate **4** (light blue curve), whereas the cells that were incubated with conjugate **3** (SWNT-biotin,

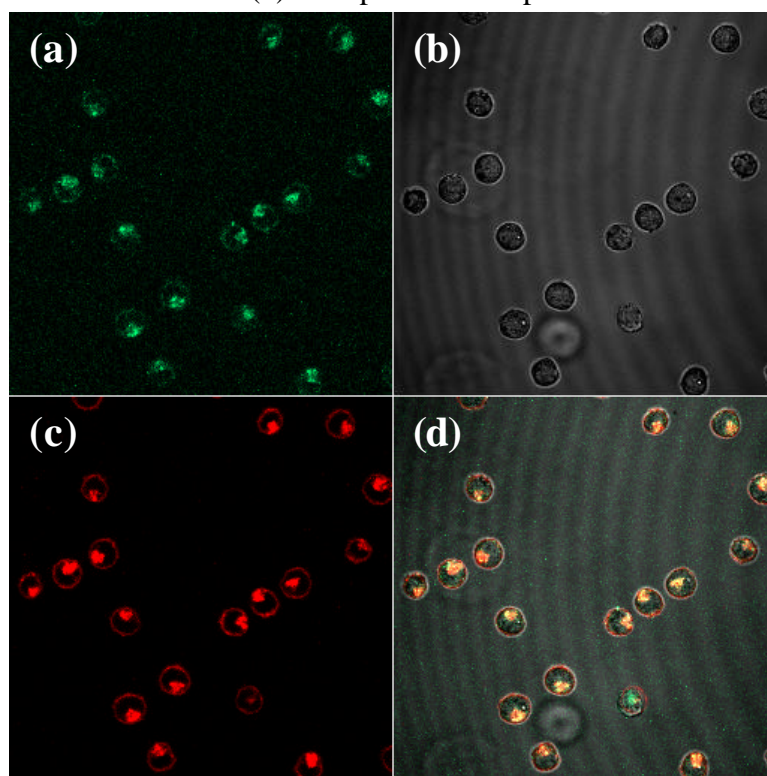
no SA, dark blue curve) showed a minimum level of cell death similar to the untreated cells (red curve). These results further confirm that the nanotubes themselves (and SWNT-biotin conjugates) do not affect cell viability, and that the extensive cell death observed after exposure to conjugate **4** is due to the large amount of internalized streptavidin. We also carried out an additional incubation of the HL60 cells with conjugate **4**, for longer period of times. As shown in S_Figure 4, after a five-hour long incubation, dramatically higher level of PI staining can be observed from the cells (light green curve).

Effects of Nanotube Concentration to the Internalization of SA and Cell Viability.

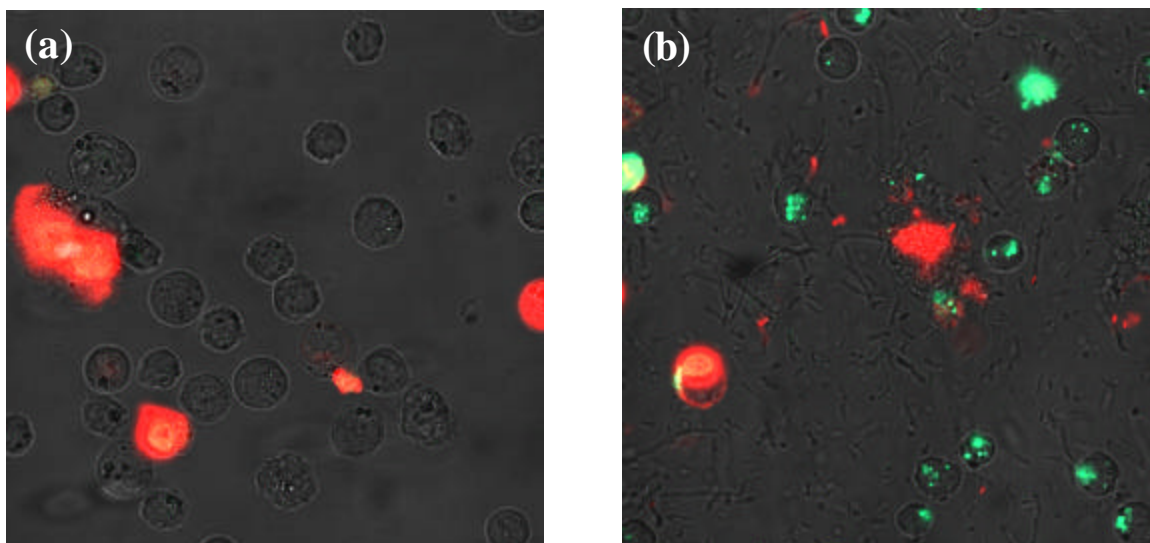
We carried out a set of incubations with conjugate **4**, for which the [SA] was kept constant at 2.5 μ M, while the [SWNT] was varied from 0.01 – 0.2 mg/ml. Viability of the cells was examined immediately following the incubation. As shown in S_Figure 5, the level of the PI staining detected appears insensitive to the concentration of nanotubes for [SWNT] >0.05 mg/ml. This is consistent with the observation that the amount of nanotubes in this concentration range is in excess relative to proteins, and the amount of proteins carried inside cells are on the same order for the different nanotube concentrations. Cell death is reduced for low [SWNT] =0.01 and 0.025 mg/ml, since the loading of proteins onto the dilute tube solution is reduced from the [SWNT]>0.05 mg/ml cases. These results also indicate that increases in nanotubes concentration do not cause more cell death in the range studied.



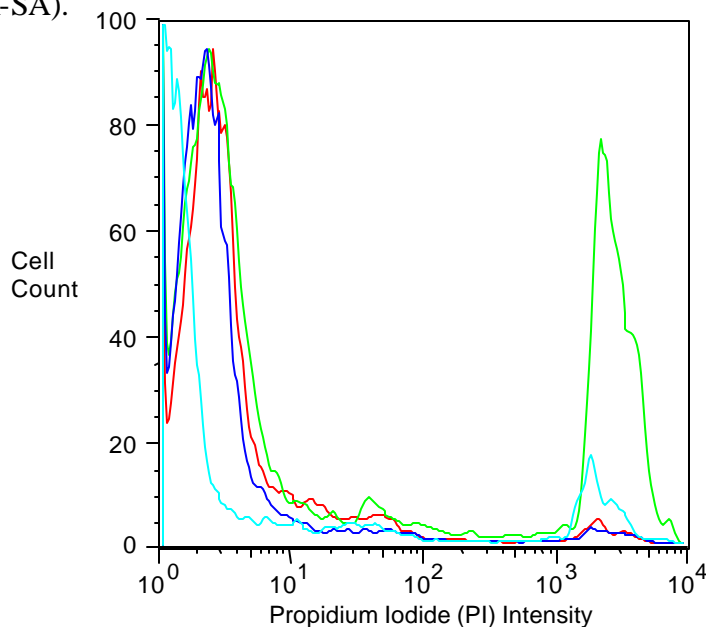
S_Figure 1. Nanotube characterization. (a) An AFM image of the oxidized and cut SWNT 1. Scale bar = 300 nm. (b) Zeta potential vs. pH for the nanotubes.



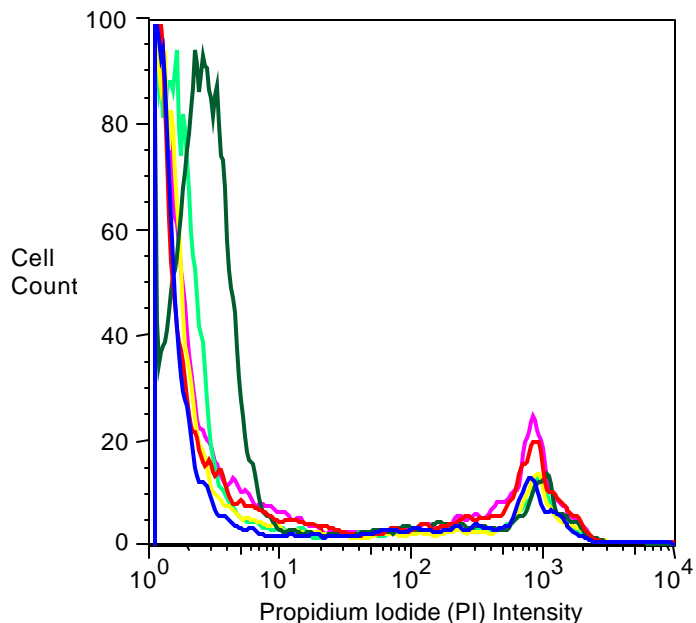
S_Figure 2. Staining of endosomes formed around nanotube conjugates reveals endocytosis. Confocal images of HL-60 cells taken after hour-long incubation with both conjugate 4 (SWNT-biotin-SA) and the red marker FM 4-64. Confocal detection of (a) green fluorescent 4 inside cells (b) bright-field image of cells (c) red endocytosis vesicles (endosomes) inside cells stained by FM 4-64 and (d) overlap of (a)-(c), indicating that conjugate 4 (green) is being internalized via endocytosis (red), indicated by yellow color.



S_Figure 3. Cell viability studies of HL60 cells. Confocal images of HL60 cells taken 48 h after hour-long incubation with (a) conjugate **3** (SWNT-biotin) and (b) conjugate **4** (SWNT-biotin-SA).



S_Figure 4. Cell viability studies of HL60 cells. The cells are stained with PI prior to analysis, and viability is assessed by the level of PI observed from the cells, immediately after incubation. Cell cytometry data obtained immediately from untreated cells (red), cells treated with conjugate **3** (SWNT-biotin, dark blue) and cells treated with conjugate **4** (SWNT-biotin-SA) for 1 h (light blue) and cells treated with conjugate **4** for 5 h (light green). The peak observed at low PI intensity ($\leq 10^1$) is due to the background fluorescence from the cells themselves. Peaks observed at PI intensity $> 10^1$, however, indicate detection of PI from the cells, therefore denoting cell death. High level of PI staining ($\sim 10^3$) can already be observed immediately after incubation from the cells exposed to the conjugate **4**, whereas cells exposed to conjugate **3** exhibited cell death level comparable to that of the untreated cells.



S_Figure 5. Cell viability studies of HL60 cells after incubation with conjugate **4**. The [SA] in the incubation mixture was kept constant at 2.5 μM , while the [SWNT] was varied. Cell cytometry data was obtained immediately from untreated cells (dark green), cells treated with conjugate **4** with [SWNT] = 0.01 mg/ml (blue), 0.025 mg/ml (light green), 0.05 mg/ml (yellow), 0.1 mg/ml (red) and 0.2 mg/ml (pink). The cells are stained with PI prior to analysis. As mentioned in S_Figure 4, the peak detected from the histogram at PI level $\leq 10^1$, is a measure of the auto-fluorescence from the cells themselves. The level of the PI staining detected ($> 10^1$, indicating cell death) appears insensitive to the concentration of nanotubes in the range varied. This is consistent with that the amount of nanotubes in this concentration range is in excess relative to proteins, and the amount of proteins carried inside cells is approximately similar for the different nanotube concentrations. This result also indicates that increases in nanotube concentration do not cause more cell death in the range studied.